

ARTICLE TYPE

N-alpha-Aminoacyl Colchicines as Promising Anticancer Agents

Ana Marzo-Mas^a, Laura Conesa-Milián^a, Sam Noppen^b, Sandra Liekens^b, Eva Falomir^{*a}, Juan Murga^a, Miguel Carda^a, J. Alberto Marco^c

^aDepartamento de Química Inorgánica y Orgánica, Univ. Jaume I, E-12071 Castellón, Spain; ^bLaboratorium Virologie en Chemotherapie (Rega Instituut), Rega - Herestraat 49 - bus 1043, 3000 Leuven, Belgium; ^cDepartamento de Química Orgánica, Univ. Valencia, E-46100 Burjassot, Valencia, Spain.

ARTICLE HISTORY

Received:
Revised:
Accepted:

DOI:

Abstract: Background: In the last years, many efforts have been made to find colchicine derivatives with reduced toxicity. Additionally, the deregulation of amino acids uptake by cancer cells provides an opportunity to improve anticancer drug effectiveness. **Objective:** To design new colchicine derivatives with reduced cytotoxicity and enhanced selectivity by means of introducing aminoacyl groups. **Method:** 34 colchicine analogues bearing L- and D-amino acid pendants were synthesized and characterized by NMR, IR and MS techniques. Cytotoxicity and antimetabolic properties were assessed by spectrophotometry and cell cycle assays. Oncogene downregulation was studied by RT-qPCR whereas in vivo studies were performed in SCID mice. **Results:** Compounds exhibit high antiproliferative activities at the nanomolar level while being, in general, less cytotoxic than colchicine. Most compounds inhibit the polymerization of tubulin in a way similar to colchicine itself, with L-amino acid derivatives being the most active in the inhibition of tubulin polymerization. All selected compounds caused cell cycle arrest at the G2/M phase when tested at 1 μ M. More specifically, Boc-L-proline derivative **6** arrested half of the population and showed one of the highest Selectivity Indexes. Derivatives **1** (Boc-glycine), **27** (D-leucine) and **31** (Boc-glycine-glycine) proved fairly active in downregulating the expression of the c-Myc, hTERT and VEGF oncogenes, with compound **6** (Boc-L-proline) having the highest activity. This compound was shown to exert a potent anti-tumor effect when administered intraperitoneally (LD₅₀ > 100 mg/kg for **6**, compared with 2.5 mg/kg for colchicine). **Conclusion:** Compound **6** offers an opportunity to be used in cancer therapy with less toxicity problems than colchicine.

Keywords: colchicine, L- and D- amino acid, cancer, non-toxic, cell cycle, tubulin, in vivo, oncogene downregulation.

1. INTRODUCTION

The mitotic spindle is the biological structure generated in eukaryotic cells during the mitosis process. This cytoskeletal structure separates chromatids into daughter cells during cell division. The spindle is constituted of hundreds of proteins, being tubulin one of the most important. Tubulin is a heterodimeric protein formed by the non-covalent binding of two very similar globular proteins called α - and β -tubulin. The polymerization process of tubulin generates the microtubules, which are tubular structures in a continuous state of formation and disruption. This complex dynamic behavior let the cell to quickly assemble or disassemble microtubule structures and is essential to pull apart eukaryotic chromosomes [1]. Antimitotic drugs disrupt microtubule dynamics and activate the spindle assembly checkpoint, arresting cell cycle progression in the mitosis phase, with subsequent cell death. Drugs that bind to the vinca and colchicine sites at β -tubulin are classified as destabilizing drugs, as they inhibit the polymerization of microtubules [2].

Colchicine is a fat-soluble natural alkaloid derived from

plants such as *Colchicum autumnale* and *Gloriosa superba* [3]. It is used as a medicine in the treatment of acute and recurrent gouty arthritis, familial Mediterranean fever and secondary amyloidosis among other diseases [4]. Its anti-inflammatory effects may be, among others, due to its antimetabolic capacity by interfering in the assembly of the cytoskeleton through the reversible and selective binding to tubulin [5]. Moreover, recent studies have pointed out that the anti-inflammatory effect of colchicine may be also due by changes at transcriptional level. In this sense, Ben-Chetrit found that colchicine was able to suppress many genes related to the inflammation process and many others related to cell cycle regulation. The handicap was that colchicine cannot clinically be used in cancer treatments due to its relatively narrow therapeutic index [6]. Many efforts have been made to find more effective and less toxic colchicine derivatives by modifying its structure so some derivatives of colchicine, such as thiocolchicoside (NeoflaxTM, MuscorilTM) are being used as anti-inflammatory and analgesic drugs. Another example is the benzyl derivative depicted in Figure 1, which involves the formal substitution of the colchicine acetyl group by the 3,4-difluorobenzyl group. This structural change provides

*Address correspondence to this author at the Química Inorgánica y Orgánica dept, Universitat Jaume I, E-12071, Castellón, Spain; E-mail: efalomir@uji.es

improved biological activity in vitro against sensitive and resistant cancer cells [7].

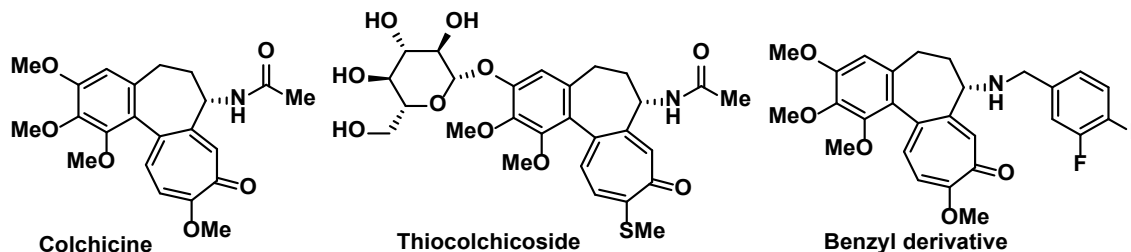


Figure 1. Colchicine derivatives.

This lack of selectivity for cancer cells versus healthy ones is not exclusive of colchicine but occurs in most antiproliferative agents used in cancer chemotherapy. In fact, in the last years, the emphasis in anticancer drug development has been shifting from cytotoxic nonspecific agents to targeted compounds towards one or more of the ten hallmarks of cancer cells [8]. Many biomolecules are endowed with these hallmarks, for example upregulation of c-MYC, a transcription factor that plays a major role in the increased proliferative activity. Moreover, deregulation of c-MYC correlates with upregulation of VEGF, which is involved in angiogenesis, and with hTERT expression, which is related to telomerase activation [9].

Recently, not only targeting but also delivery have been receiving special attention in order to enhance anticancer drug efficacy. One of the hallmarks of cancer cells is the deregulation of cellular metabolism so that among these cancer-associated metabolic changes, deregulated uptake of amino acids and use of opportunistic modes of nutrient acquisition stand out.

For the last five years we have been working in the search of anticancer agents with selective cotargeting of multiple cancer hallmarks. In this sense, we designed, synthesized and studied some hybrid molecules with a colchicine moiety and a pironetin analogue fragment. We found that, in addition to binding to tubulin, these compounds were able to downregulate the expression of some oncogenes such as c-MYC, hTERT and VEGF. These three genes are of paramount importance in the cancer generation process. Our results pointed to the colchicine fragment being responsible for the observed biological activities, even though high doses were required in certain cases (50 nM-15 μ M) [10].

Since colchicine is not only able to target tubulin but also to downregulate some oncogene expression, we decided to

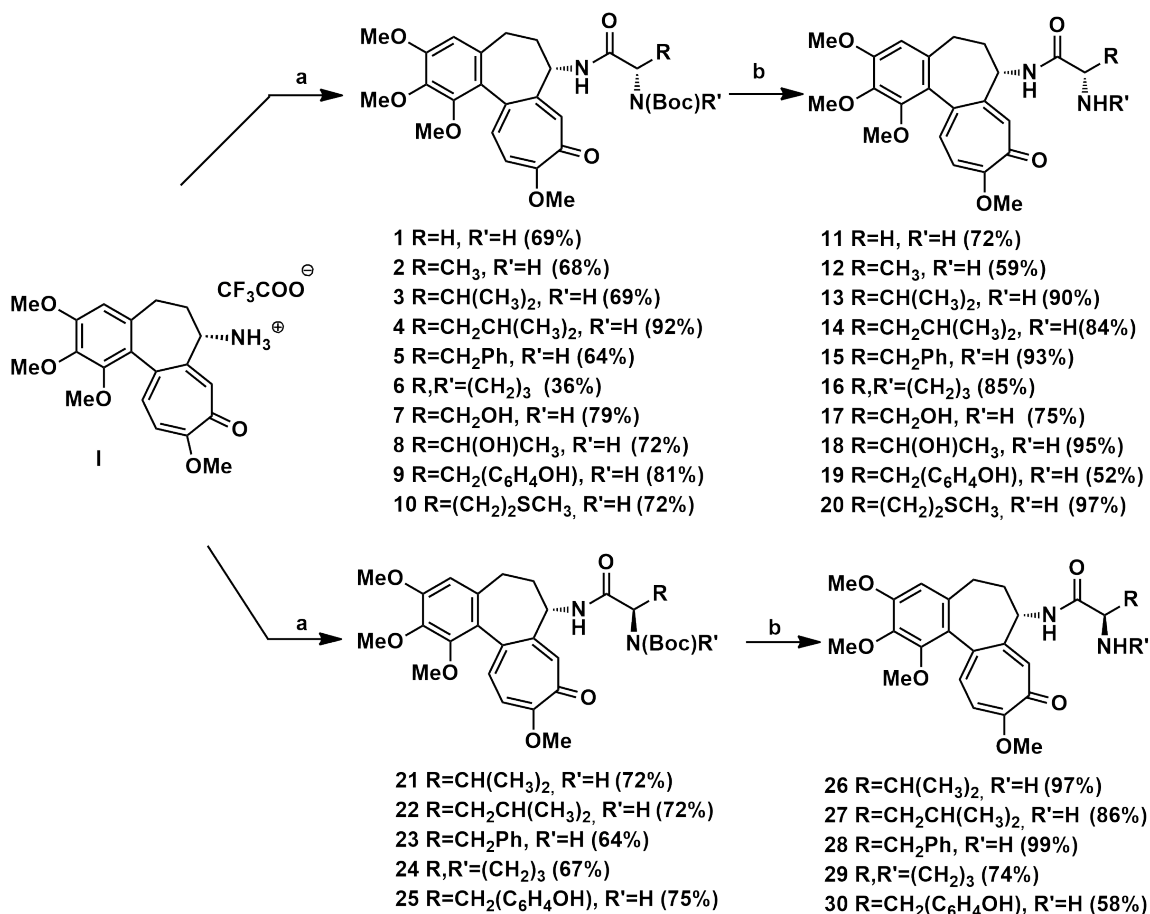
design new colchicine derivatives with reduced cytotoxicity and enhanced selectivity. One of our strategies was to take advantage of the deregulation of amino acid uptake in cancer cell to conjugate the amino group of deacetylcolchicine with different amino acids [11]. To extend our research on colchicine derivatives with potential utility in cancer therapy and based on the aforementioned aspects, we have prepared the aminoacyl derivatives depicted in Schemes 1 and 2, in which the *N*-acetyl residue of colchicine has been replaced by various aminoacyl moieties.

Our purpose was to assess the effects on biological activity caused by the introduction of these aminoacyl groups.

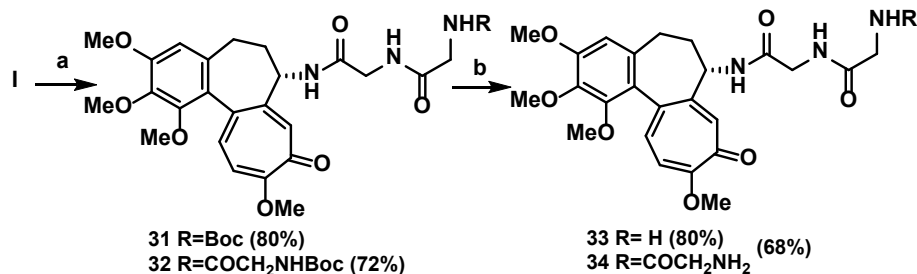
2. MATERIALS AND METHOD

2.1. Synthetic Work

The trifluoroacetate salt of *N*-deacetyl colchicine (**I**) [12] was used as starting material to prepare the aminoacyl derivatives. Scheme 1 depicts the preparation of colchicine derivatives with L-amino acid pendants. Thus, treatment of **I** with the corresponding *N*-Boc protected L-amino acid in the presence of EDCI·HCl and DMAP in DMF afforded *N*-Boc protected derivatives **1-10**, with fair to good yields [13]. Reaction of these *N*-Boc derivatives with Amberlyst-15 resin [14], followed by treatment with methanolic ammonia, gave rise to aminoacyl derivatives **11-20**. Scheme 1 also depicts the preparation of aminoacyl derivatives bearing D-amino acid pendants by means of using the same synthetic route as before. In addition, we have also prepared Gly-Gly and Gly-Gly-Gly derivatives depicted in Scheme 2. Details about the precise reaction conditions are indicated in the Supplementary Material as well as the analytical NMR data and graphical spectra.



Scheme 1. Reagents and conditions: (a) (L)- or (D)-RCH(NHBoc)COOH, EDCI·HCl, DMAP, DMF, from 0°C to rt. (b) Amberlyst 15 resin, CH₂Cl₂, rt, 24 h, then 4M NH₃ in MeOH, 1 h, rt.



Scheme 2. Reagents and conditions: (a) Boc-Gly-Gly-OH or Boc-Gly-Gly-Gly-OH, EDCI·HCl, DMAP, DMF, from 0°C to rt. (b) Amberlyst 15 resin, CH₂Cl₂, rt, 24 h, then 4M NH₃ in MeOH, 1 h, rt.

2.2. Biological Assays

2.2.1. Cell Culture

Cell culture media were purchased from Gibco (Grand Island, NY). Fetal bovine serum (FBS) was obtained from Harlan-Seralab (Belton, U.K.). Supplements and other chemicals not listed in this section were obtained from Sigma Chemical Co. (St. Louis, MO). Plastics for cell culture were supplied by Thermo Scientific BioLite. All tested compounds were dissolved in DMSO at a concentration of 10 mM and stored at -20°C until use. HT-29, MCF-7, A549 and HEK-293 cell lines were maintained in Dulbecco's modified Eagle's medium (DMEM) containing glucose (1 g/L), glutamine (2 mM), penicillin (50 µg/mL), streptomycin (50 µg/mL), and amphotericin B (1.25 µg/mL), supplemented with 10% FBS.

2.2.2. Cell Proliferation Assay

In 96-well plates 5×10^3 HT-29, MCF-7, A549 or HEK-293 cells per well were incubated with serial dilutions of the tested compounds in a total volume of 100 µL of growth media. The 3-(4,5-dimethylthiazol-2-yl)-2,5-diphenyl-tetrazolium bromide (MTT; Sigma Chemical Co.) dye reduction assay in 96-well microplates was used, as previously described [15]. After 2 days of incubation (37 °C, 5% CO₂ in a humid atmosphere), 10 µL of MTT (5 mg/mL in phosphate-buffered saline, PBS) was added to each well, and the plate was incubated for a further 3 h (37 °C). Then, the supernatant was discarded and replaced by 100 µL of DMSO to dissolve formazan crystals. The absorbance was then read at 540 nm by spectrophotometry. For all concentrations of compound, cell viability was expressed as the percentage of

the ratio between the mean absorbance of treated cells and the mean absorbance of untreated cells. Three independent experiments were performed, and the IG_{50} values (i.e., concentration half inhibiting cell proliferation) were graphically determined using GraphPad Prism 4 software.

2.2.3. Tubulin Self-assembly Measurements

Purified tubulin was used for these measurements. Tubulin polymerization was carried out in a 96 well plate. In each well 50 μ L of a solution of 25 μ M of tubulin in GAB buffer was added to 50 μ L of 27.5 μ M solution of the corresponding compounds in GAB buffer (20 mM sodium phosphate, 10 mM $MgCl_2$, 1 mM EGTA, 30% glycerol) and 0.1 mM GTP at pH = 6.5. Then, the plate was incubated at 37 °C in Multiskan® and absorbance at 340 nM was registered every 30 seconds for 2 hours.

2.2.4. Cell Cycle Analysis

Progression of the cell cycle was analysed by means of flow cytometry with propidium iodide. After incubation with compounds for 24 h, A549 cells were fixed, treated with RNase and stained with propidium iodide following instructions of BD Cycletest™ DNA Kit. Analysis was performed with a BD Accuri™ C6 flow cytometer.

2.2.5. RT-qPCR Assay

HT-29 cells at 70-80% confluence were collected and 1.5×10^5 cells were placed in a six well plate in 1.5 mL of medium. After 24 h, cells were incubated with the corresponding compounds for 48 h. Cells were collected and the total cellular RNA from HT-29 cells was isolated using Ambion RNA extraction Kit according to the manufacturer's instructions. The cDNA was synthesized by MMLV-RT with 1-21 μ g of extracted RNA and oligo(dT) 15 according to the manufacturer's instructions. Genes were amplified by use of a thermal cycler and StepOnePlus™ Taqman® probes. TaqMan® Gene Expression Master Mix Fast containing the appropriate buffer for the amplification conditions, dNTPs, thermostable DNA polymerase enzyme and a passive reference probe was used. To amplify each of the genes the predesigned primers were used and sold by Life Technologies TaqMan® Gene Expression Assays, Hs99999903-m1 (β -actin), Hs00972646-m1 (hTERT), Hs00153408-m1 (c-MYC) and Hs00900055-m1 (VEGF-A).

2.2.6. In Vivo Studies

Human metastatic breast cancer xenografts were established as previously described [16]. The luciferase-positive LM2 lung metastatic cell line (MDA-MB-231 clone 4715) was a kind gift of Prof. Massagué [17]. Female severe combined immunodeficient (SCID) mice were used at the age of 8 weeks. LM2 cells (10^6) were suspended in 50% matrigel (BD Biosciences) in PBS and injected in the mammary fat pad of anesthetized SCID mice. When tumors were around 100 mm^3 in size, compound **6** was injected intraperitoneally (i.p.) at 75 mg/kg in PBS containing 5% DMSO and 20%

cremophor. Control mice received only 5% DMSO, 20% cremophor in PBS. Tumor growth was measured with an IVIS Spectrum imaging system (Caliper Life Sciences, Hopkinton, MA, USA). Before imaging, mice were anesthetized and injected subcutaneously with 150 mg/kg luciferin. Images were recorded every 2 minutes and maximum radiance values (photons/sec) were retained. Lung metastasis was determined after shielding the primary tumor with a black paper. Tumor size was measured using a digital caliper and calculated with the following formula: tumor volume (mm^3) = $0.5 \times a \times X \times b^2$, where a is the longest diameter and b is the shortest diameter.

2.2.6. Statistics studies

The statistical significance was evaluated using one-sample t-tests ($P < 0.01$) using GraphPad® software.

3. RESULTS AND DISCUSSION

3.1. Inhibition of Cell Proliferation

The MTT assay was used to establish the capacity of compounds **1-34** to inhibit cell proliferation by means of their IG_{50} values towards the tumor cell lines HT-29 (human colon adenocarcinoma), MCF-7 (breast adenocarcinoma), A549 (human alveolar lung epithelial carcinoma cells) as well as towards the non-tumor cell line HEK-293 (human embryonic kidney cells). The results were compared with those of colchicine and are depicted in Table 1 along with the calculated selectivity indexes SI_A (for HT-29 cell line), SI_B (for MCF-7 cell line) and SI_C (for A549 cell line), obtained by dividing the IG_{50} values of the non-tumor cell line (HEK-293) by those of the corresponding tumor cell line. The SI is a calculated parameter that helps to estimate the possible selectivity of compounds for cancer cells vs. non cancer ones. Thus, a higher SI value indicates a higher therapeutic safety margin.

The majority of *N*-aminoacyl derivatives of colchicine present IG_{50} values in the medium to low nanomolar range in the tumor cell lines. In the HT-29 cell line, compounds **1**, **12**, **16**, **27**, **28** and **31** display a higher antiproliferative activity than colchicine itself. In the MCF-7 cell lines derivatives **1**, **3**, **16**, **22** and **27** are those showing higher antiproliferative capacities. As for the A549 cell line, none of the derivatives reaches the high antiproliferative capacity shown by the natural alkaloid. Interestingly, the majority of the synthetic derivatives exhibit SI (selectivity indexes) values greater than colchicine with L-proline derivative **16**, D-Boc-valine **21**, D-Boc-leucine **22**, D-leucine **27** and D-phenylalanine **28** showing the highest SI values. Indeed, the most selective derivatives are **16** (L-Proline) and **27** (D-Leucine), which present a SI_B value higher than 100 and 200, respectively, thus more than 200 times higher than colchicine. These synthetic compounds therefore could offer the possibility for use in cancer therapy with lower dosages and less acute toxicity problems than in the case of colchicine.

Table 1. IG_{50} values (nM) of synthetic compounds **1-34** in cancer cell lines HT-29, MCF-7 and A549 and one non-cancer cell line HEK-293. IG_{50} values are expressed as the compound concentration (nM) that inhibits the cell growth by 50%. Data are the average (\pm SD) of three experiments. $^{a}SI_A = IG_{50}(\text{HEK-293})/IG_{50}(\text{HT-29})$. $^{b}SI_B = IG_{50}(\text{HEK-293})/IG_{50}(\text{MCF-7})$. $^{c}SI_C = IG_{50}(\text{HEK-293})/IG_{50}(\text{A549})$.

Compound	HT-29	MCF-7	A549	HEK-293	SI_A^a	SI_B^b	SI_C^c
Colchicine	50 \pm 3	12 \pm 7	12.2 \pm 0.7	5 \pm 1	0.1	0.4	0.4
1	8.5 \pm 0.8	8.8 \pm 0.9	21.0 \pm 2.2	13.6 \pm 0.5	1.6	1.6	0.6
2	139 \pm 25	37 \pm 4	61 \pm 24	45 \pm 7	0.3	1.2	0.7
3	61 \pm 5	1.2 \pm 0.1	105 \pm 16	0.8 \pm 0.1	0.01	0.7	0.01
4	238 \pm 21	1600 \pm 300	800 \pm 160	240 \pm 30	1	0.2	0.3
5	100 \pm 13	1150 \pm 40	770 \pm 14	15 \pm 4	0.2	0.01	0.02
6	80 \pm 3	44 \pm 6	38 \pm 3	150 \pm 10	2	3	4
7	62 \pm 3	67.6 \pm 1.4	60 \pm 15	63.4 \pm 0.3	1	1	1
8	100 \pm 5	161 \pm 11	230 \pm 80	170 \pm 40	2	1	1
9	716.9 \pm 0.5	300 \pm 30	550 \pm 50	2600 \pm 300	4	9	5
10	81 \pm 3	160 \pm 30	69 \pm 5	150 \pm 12	2	1	2
11	94 \pm 6	67 \pm 14	365 \pm 24	300 \pm 30	3	5	1
12	41 \pm 3	55 \pm 3	52 \pm 4	131.0 \pm 0.5	3	2	3
13	84 \pm 8	85 \pm 12	204 \pm 4	398 \pm 25	5	5	2
14	278 \pm 14	400 \pm 32	120 \pm 30	980 \pm 60	4	2	8
15	181 \pm 43	240 \pm 51	370 \pm 23	470 \pm 30	3	2	1
16	23 \pm 4	3.3 \pm 0.3	110 \pm 19	790 \pm 30	34	239	7
17	166 \pm 7	1140 \pm 60	1419 \pm 4	2900 \pm 80	17	2	2
18	138 \pm 11	340 \pm 40	1107 \pm 12	1510 \pm 6	10	4	1
19	116 \pm 20	86 \pm 18	750 \pm 80	1600 \pm 100	14	14	2
20	50 \pm 5	139 \pm 19	130 \pm 30	272 \pm 24	5	2	2
21	238 \pm 10	30 \pm 4	280 \pm 70	2000 \pm 1000	9	67	7
22	125 \pm 7	5.5 \pm 1.1	230 \pm 30	360 \pm 30	3	65	2
23	158 \pm 24	1920 \pm 30	220 \pm 60	660 \pm 40	4	0.3	3
24	114.6 \pm 2.3	63 \pm 12	82 \pm 26	110 \pm 10	1	2	1
25	458 \pm 3	790 \pm 70	900 \pm 200	1660 \pm 110	4	2	2
26	295 \pm 38	80 \pm 10	430 \pm 40	20 \pm 3	0.1	0.2	0.05
27	31 \pm 3	3.3 \pm 0.3	106 \pm 13	390 \pm 30	13	118	4
28	10.3 \pm 2.5	82.0 \pm 2.0	230 \pm 90	350 \pm 30	34	4	2
29	112.1 \pm 2.1	88 \pm 21	250 \pm 60	690 \pm 50	6	8	3
30	460 \pm 10	1100 \pm 300	690 \pm 40	3400 \pm 300	7	3	5
31	39 \pm 5	51.9 \pm 1.2	70 \pm 19	150 \pm 40	4	3	2
32	129 \pm 8	341 \pm 17	710 \pm 40	415 \pm 24	3	1	1
33	531 \pm 23	2400 \pm 210	2000 \pm 400	810 \pm 40	2	0.3	0.4
34	480 \pm 50	460 \pm 60	1900 \pm 100	610 \pm 60	1	1	0.3

3.2. Effect on Tubulin Assembly

The effects of our derivatives on tubulin self-assembly was established by means of the critical concentration, that is the concentration of tubulin in the equilibrium stage. Thus, microtubule formation was carried out in glycerol-assembling buffer (GAB) in the presence of compounds **1-34**, as well as colchicine and podophyllotoxin, as a positive control

inhibitors. A solution of 25 μ M tubulin was incubated at 37°C with 27.5 μ M concentrations of colchicine, podophyllotoxin and compounds **1-34**. Table 2 displays the results achieved.

Table 2. Critical Concentration (CrC) for the assembly of purified tubulin in GAB in the presence of colchicine, podophyllotoxin and the colchicine analogues **1-34**. Data are the average (\pm SD) of three experiments.

Compound	CrC (μM)	Compound	CrC (μM)
Control	9 \pm 2	17	23 \pm 1
Colchicine	24 \pm 1	18	23 \pm 1
Podophyllotoxin	23 \pm 1	19	22 \pm 1
1	23 \pm 1	20	23 \pm 1
2	24 \pm 1	21	22 \pm 1
3	21 \pm 2	22	21 \pm 2
4	17 \pm 5	23	21 \pm 1
5	22 \pm 1	24	16 \pm 1
6	13 \pm 1	25	22 \pm 1
7	23 \pm 1	26	21 \pm 3
8	23 \pm 1	27	22 \pm 1
9	21 \pm 1	28	22 \pm 1
10	24 \pm 1	29	14 \pm 1
11	23 \pm 1	30	20 \pm 1
12	23 \pm 1	31	6 \pm 2
13	23 \pm 1	32	18 \pm 1
14	21 \pm 2	33	24 \pm 1
15	23 \pm 1	34	23 \pm 1
16	21 \pm 1		

As expected, colchicine and podophyllotoxin, both well-known microtubule-destabilizing agents, increase the critical concentration value from 9 μM in the absence of the drugs (DMSO vehicle) to a value of 24.5 μM for colchicine and 23.5 μM for podophyllotoxin. All derivatives, except for compound **31** (Boc-Glycine-Glycine), inhibit the formation of microtubules as they are able to increase the critical concentration of tubulin. Indeed, these critical concentration values of analogues **1–34** (except for **31**) confirm that the observed antiproliferative effect in cells is due to their interaction with tubulin.

Figure 2 depicts the effects of the L- α -amino acids derivatives on the kinetics of tubulin self-assembly. As it can be observed, the majority of the synthesized compounds showed a full inhibition of microtubule formation, as does colchicine (CLC hereafter).

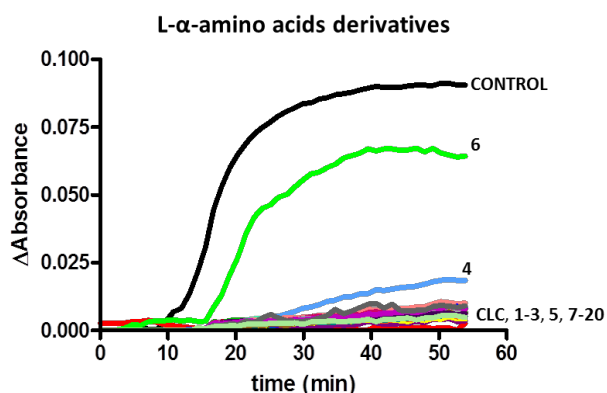


Figure 2. Effects of colchicine and compounds **1–20** on the kinetics of tubulin assembly. The lines in the figure show the turbidity time course of polymerization of tubulin alone (black) at 25 μM , colchicine (red) and all the compounds such as **4** (blue) and **6** (green). All compounds were at 27.5 μM .

In general terms, it may be concluded that L- α -amino acids derivatives are the most active drugs. Within this subgroup, compounds having a small hydrophobic residue (**1**, **2**, **11** and **12**) or a polar group (**7**, **8**, **10**, **17**, **18** and **20**) show critical concentration values close to those of colchicine. However, derivatives having a large bulky residue (**4** and **6**) can be classified as partial inhibitors of tubulin polymerization.

The effects of the D- α -amino acids derivatives and the dipeptide and tripeptide of glycine derivatives on the kinetics of tubulin self-assembly are summarized in Figure 3.

D- α -amino acids and Gly-Gly and Gly-Gly-Gly derivatives

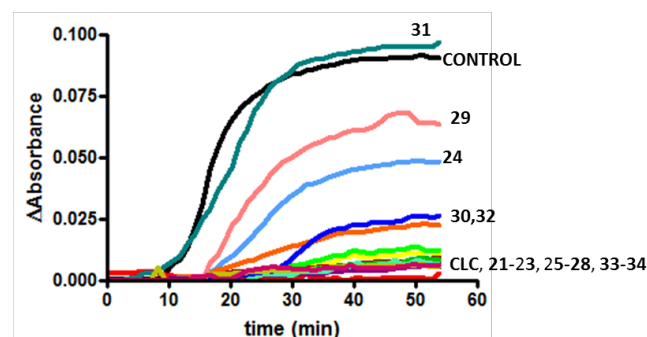


Figure 3. Effects of colchicine and compounds **21–34** on the kinetics of tubulin assembly. The lines in the figure show the turbidity time course of polymerization of tubulin alone (black) at 25 μM , colchicine (red) and all the compounds such as **24** (blue), **29** (pink), **30** (orange), **31** (grey) and **32** (deep blue). All compounds were at 27.5 μM .

The majority of drugs are able to inhibit the tubulin polymerization process, as does colchicine. As indicated above, compound **31** scarcely affects the tubulin polymerization process. Interestingly, derivatives having a large bulky residue (**24**, **29**, **30** and **32**) caused partial inhibition of microtubule formation and also a delay on the polymerization process.

In order to quantify this delay of the nucleation and elongation process, we have calculated the I_{t50} values in each case, which is defined as the time needed to reach 50% of the polymerization equilibrium. Mathematically, the I_{t50} value coincides with the inflection point of the sinusoidal curve that comes from the kinetics of tubulin assembly in each case. The I_{t50} values obtained for the control (DMSO) and compounds **24** (D-Boc-proline), **29** (D-proline), **30** (D-phenylalanine) and **32** (Boc-Gly-Gly-Gly), along with derivatives **4** (L-Boc-leucine) and **6** (L-Boc-Proline), are shown in Table 3.

Table 3. I_{t50} of selected N-aminoacyl derivatives for tubulin self-assembly. Data are the average (\pm SD) of three experiments.

Compound	I_{t50} (min)
Control	16 \pm 1
4	29 \pm 9
6	22 \pm 1
24	26 \pm 1
29	24 \pm 1
30	27 \pm 3
32	32 \pm 1

Compounds having a comparatively high value of critical concentration with respect to the control (lower absorbance in the stationary phase) and a higher I_{t50} value with respect to the

control (increased time required for nucleation and elongation) are considered as partial inhibitors of the polymerization of tubulin.

3.3. Effect on the Cell Cycle

As all but one (compound **31**) of our colchicine derivatives prevent in vitro microtubule assembly, it was convenient to establish whether they also could inhibit microtubule polymerization inside cells causing cell cycle arrest and to characterize their effects on microtubules, mitosis and DNA content. First of all, we performed a selection of the most active compounds by studying the effects on the morphology

of the cells after 24 h treatment with different concentrations of our compounds. In the presence of colchicine and compounds **1**, **7**, **15**, **17** and **21**, most of the A549 cells became rounded mitotic cells as compared with the control cells [18], which were spread epithelial-like adherent cells with few mitotic cells. This effect was not observed in the presence of compounds **2-5**, **8**, **9-11**, **13**, **18**, **20**, **23-26**, **30**, **32** and **33**, hence, they were discarded. Next, in order to establish the cell cycle distribution into the different phases, A549 cells were treated for 24 hours with colchicine and the aforementioned compounds. The main results are summarized in Table 4.

Table 4. Cell cycle distribution for colchicine and selected compounds. Data are the average (\pm SD) of three experiments.

Compound	Conc. (μ M)	Sub G1	G1	S	G2/M
Control		2 \pm 1	73 \pm 3	15 \pm 6	11 \pm 4
Colchicine	0.050	3 \pm 1	27 \pm 14	11 \pm 2	59 \pm 17
1	1	8 \pm 1	25 \pm 1	16 \pm 1	50 \pm 1
6	0.1	3 \pm 1	35 \pm 2	15 \pm 2	47 \pm 5
7	1	10 \pm 1	21 \pm 2	10 \pm 1	51 \pm 1
9	0.5	1.0 \pm 0.4	50 \pm 7	4 \pm 1	45 \pm 2
12	0.05	4 \pm 1	56 \pm 3	16 \pm 4	24 \pm 5
14	0.1	3 \pm 1	56 \pm 2	7 \pm 2	39 \pm 3
15	1	6 \pm 1	19 \pm 1	11 \pm 1	62 \pm 3
16	0.1	1.0 \pm 0.5	66 \pm 4	15 \pm 5	23 \pm 6
17	15	3 \pm 2	31 \pm 16	18 \pm 3	47 \pm 15
19	0.5	2 \pm 1	45 \pm 5	17 \pm 4	36 \pm 3
21	0.5	6 \pm 3	30 \pm 2	14 \pm 3	49 \pm 2
22	0.1	1.0 \pm 0.2	29 \pm 6	10 \pm 2	60 \pm 8
27	0.1	3 \pm 1	34 \pm 2	18 \pm 5	44 \pm 7
28	0.2	2 \pm 1	33 \pm 4	11 \pm 3	54 \pm 9
29	0.2	5 \pm 2	56 \pm 6	14 \pm 2	25 \pm 5
31	0.1	3 \pm 1	44 \pm 7	20 \pm 6	33 \pm 2

The observed results show that all compounds are able to arrest the cell cycle at the G2/M phase, as expected for colchicine derivatives. In all cases, a sub-G1 peak, presumably of cells undergoing apoptosis, appeared. **Some of these derivatives have been studied at different concentrations in order to set the most active compounds at the lowest concentration.** Compounds **1**, **7** and **15** cause interruption of the cell cycle at the G2/M phase when tested at approximately 1 μ M. However, at 0.2 μ M concentration, derivative **1** started to accumulate cells in G2/M phase in a higher percentage than in the control situation. Interestingly, derivatives **6** (Boc-L-Proline) and **21** (Boc-D-valine) at 0.1 μ M and 0.5 μ M concentration respectively, caused mitotic arrest in half of the cell population, while presenting some of the highest SI_C (4.0 and 7.2, respectively). Thus, compounds **6** and **21** could offer the possibility to be used in cancer therapy with lower dosages and thus less acute toxicity problems than colchicine.

3.4. Effect on the Expression of c-MYC, hTERT and VEGF Genes

In order to extend our research on colchicine derivatives with potential utility in cancer therapy, we proceeded to investigate the effect they exert on the expression of c-Myc, hTERT and VEGF genes. First of all, a preliminary study was carried out by conventional PCR to qualitatively determine which compounds were able to modify the expression of these three genes after 48 h of treatment in HT-29 cell line (data not shown). This preliminary test let us select four derivatives and their minimal active concentration (see Figure 4) for a quantitative study of gene expression on the same cell line.

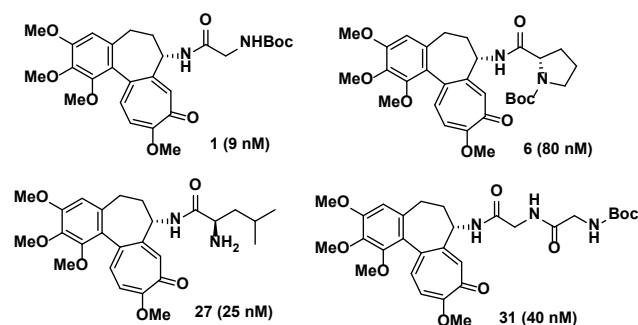


Figure 4. Selected compounds and concentrations for a quantitative gene expression test.

As regards the ability of our compounds for the inhibition of the *c-Myc* gene expression, we found that colchicine was very active at a concentration of 40 nM but has no activity when tested at 10 nM, while compound **6**, at 80 nM, was able to downregulate *c-Myc* expression to the half. In relation to *hTERT* gene expression, colchicine was able to inhibit the expression of the mentioned gene to 50% at a concentration of 40 nM, with no activity when tested at 10 nM. In this case, again compound **6** was the most active one, with **1** and **31**, at 9 and 40 nM respectively, being still more active than colchicine itself. In reference to *VEGF* gene expression, colchicine was active at a concentration of 40 nM but inactive at 10 nM. Again, compound **6** at 80 nM was found to be the most active one in inhibiting *VEGF* gene expression, with a higher activity than the natural product itself. (See Figure 5).

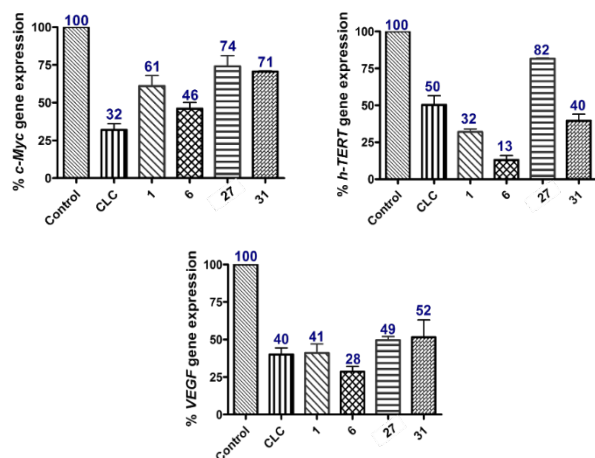


Figure 5. Expression percentage of *c-Myc*, *hTERT* and *VEGF* genes after 48 h of incubation with DMSO (control), and selected compounds (at least three measurements were performed in each case). Gene expression was normalized using β -actin as endogenous gene. Percentages above 100% indicate that the corresponding compounds were less active than the control. Error bars indicate standard errors of the mean. The statistical significance was evaluated using one-sample t-tests ($P < 0.01$).

3.5. Colchicine Derivative **6** inhibits primary tumor growth in mice

Given the good *in vitro* results obtained with compound **6**, we decided to carry out an *in vivo* study to determine its pharmacological action in a more complex biological system. To determine the *in vivo* antitumor activity of compound **6** in SCID mice, the LD_{50} value was first determined and then compared with the corresponding value for colchicine. The result was very promising as LD_{50} for compound **6** was >100 mg/kg while LD_{50} for colchicine was 2.5 mg/kg. Then, a breast cancer model was established as previously described [15]. LM2 breast cancer cells were engrafted in the mammary fat pad of SCID mice. Compound **6** was injected intraperitoneally (i.p.) at 75 mg/kg at day 17, when tumours were around 100 mm³ in size, at day 21 and at day 25. Tumor growth was significantly retarded after treatment with compound **6** as measured by bioluminescence imaging (Figure 6 A) and calliper measurement (Figure 6 D). Interestingly, already 2 hours after treatment a significant decrease in BLI was observed which is typically caused by the shutdown of blood flow after VDA treatment (Figure 6 B). This decrease was even more pronounced after 24 hours. By day 20, 72 hours after treatment with compound **6**, tumors had slightly regrown (Figure 6 B). After removal of the tumors, it was noted that the treated tumors were smaller and less vascularized (Figure 6 E). Thus, compound **6** exerts a potent antitumor effect when administered i.p.

To assess the effect of compound **6** on metastasis, the primary tumors were covered with black paper and the BLI from the lungs was measured (Figures 6 F, E). No significant difference between control and compound **6** was observed at day 34. Thus, compound **6** has no effect on the dissemination of cancer cells from the primary tumor towards the lungs. Previous reports already showed that micrometastatic tumors are resistant to anti-angiogenic therapy because no tumor vasculature is established yet and tumor cells can benefit from existing vasculature [18].

Tumor growth was measured by *in vivo* imaging until day 35. By day 18, 24 h hours after start of treatment, a dramatic decrease in luminescent signal was noted in the compound **6**-treated group whereas control tumors continued to grow (Figure 6 A). By day 20, compound **6** tumors had slightly regrown but were significantly smaller than control tumors ($p < 0.001$, Figures 6 A, C). At day 35 after cell inoculation, primary tumors were removed and the measurement of tumor size also revealed a difference between control and treated groups (Figures 6 B, D). Thus, in an early stage of tumor development, compound **6** exerts a potent anti-tumor effect when administered i.p.

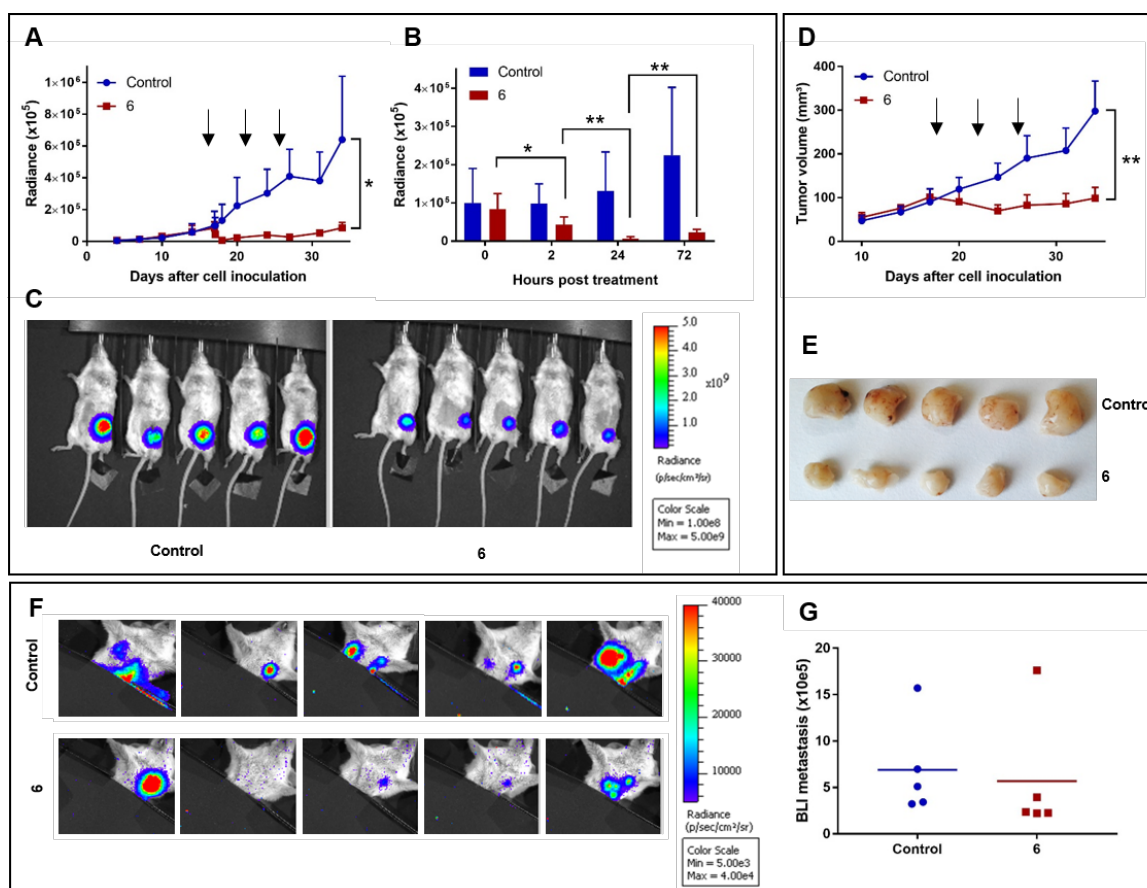


Figure 6. Intrapertoneal compound **6** impairs tumor growth but not metastasis. LM2 cells were orthotopically injected in the mammary fat pad of SCID mice. Mice were treated i.p. with compound **6** or vehicle at day 17, 21 and 25. A, B: Graphical representation of BLI signal over time emitted from the primary tumor. C: Representative bioluminescence images at day 34 are shown. D: Graphical representation of primary tumor volume evolution. E: At day 35 mice were sacrificed and pictures of dissected tumors are shown. F, G: Lung metastasis at day 34 was quantified after shielding the primary tumor. All data are mean \pm STDEV, $n = 5$. * $p < 0.05$, ** $p < 0.01$ (multiple t-test). Arrows indicate compound administration.

CONCLUSION

Colchicine analogues in which the N-acetyl residue has been replaced by some amino acid moieties have been synthesized and their antiproliferative activities towards the tumor cell lines HT-29, MCF-7 and A549 and the non-tumor cell line HEK-293 have been measured. All derivatives show IG_{50} values in the nanomolar range, being, in general, less cytotoxic than colchicine (see Table 1). In HEK-293 and A-549 cell lines all compounds exhibited IG_{50} values higher than the natural product. In HT-29 cell line, only some non-polar amino acids derivatives such as **1** (Boc-Glycine), **12** (L-Valine), **16** (L-Proline), **27** (D-Leucine), **28** (D-Phenylalanine) and **31** (Boc-Glycine-Glycine) exhibit lower IG_{50} values than the natural product. As regards MCF-7 cell line, again only some non-polar amino acids derivatives such as **1** (Boc-Glycine), **3** (Boc-L-Valine), **16** (L-Proline), **22** (Boc-D-Leucine) and **27** (D-Leucine) exhibit lower IG_{50} values than colchicine itself.

As regards the Selectivity Index (SI) values, the majority of the synthetic derivatives exhibit SI values greater than colchicine (see Figure 7). We have observed that, in general, SI values of L-Boc-amino acid derivatives are the lowest ones though they are greater than in colchicine. On the other hand, D-amino acid derivatives exhibit the highest SI. We have also observed that the glycine, leucine, proline and tyrosine derivatives exhibit the lowest toxicity values.

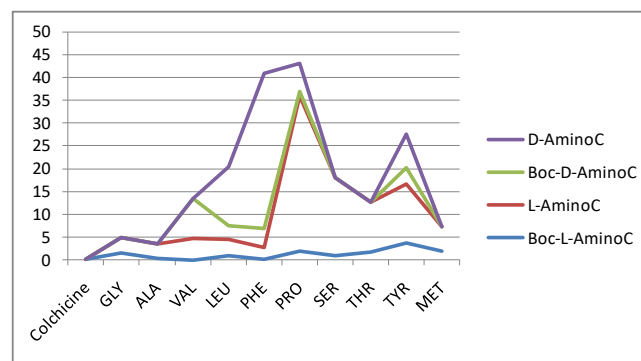


Figure 7. SI_A indexes for all colchicine derivatives.

In relation to the tubulin polymerization process, in general terms, it may be concluded that L- α -amino acids derivatives are the most active drugs. Within this subgroup, compounds having a small hydrophobic residue (**1**, **2**, **11** and **12**) or a polar group (**7**, **8**, **10**, **17**, **18** and **20**) show critical concentration values closer to that of colchicine. However, derivatives having a bulky residue (**4** and **6**) can be classified as partial inhibitors of tubulin polymerization.

On the other hand, the effects of the D- α -amino acid derivatives and Gly-Gly and Gly-Gly-Gy derivatives are also able to inhibit the tubulin polymerization process, as colchicine does. Compound **31** (Boc-Glycine-Glycine)

scarcely affects the tubulin polymerization process. Interestingly, derivatives having a large bulky residue (**24**, **29**, **30** and **32**) caused partial inhibition of microtubule formation and also a delay on the polymerization process.

The tested derivatives cause arrest of the cell cycle at the G2/M phase with concentrations higher than colchicine at 50 nM. All the selected compounds cause interruption of the cell cycle at the G2/M phase. For example, at 0.1 μ M concentration derivative **6** (Boc-L-Proline) caused the arrest of cell cycle at the half of the population, while presenting one of the highest SI_C (4.0).

As regards the effect of these compounds on the expression of oncogenes c-MYC, hTERT and VEGF, the most active derivatives were **1** (Boc-Glycine), **6** (Boc-L-Proline), **27** (D-Leucine) and **31** (Boc-Glycine-Glycine). Among them, derivative **6** is particularly outstanding as it is able to enhance the colchicine effect on the oncogene expression.

Thus, compound **6** could offer the possibility to be used in cancer therapy with less acute toxicity problems than in the case of colchicine, because it exerts a decrease in the expression of oncogenes involved in tumor aggressiveness at concentrations in which there is no antimitotic effect. The results we have obtained in the in vivo study demonstrate its antitumor efficacy and, what is even more outstanding for a colchicine derivative, its low toxicity. The deregulation of the uptake of amino acids in cancer cells plays a crucial role in the lower toxicity of amino acid conjugated colchicine derivatives, as this effect leads to a greater uptake of the derivative by the tumor cells compared to healthy ones.

LIST OF ABBREVIATIONS

A549	= human lung adenocarcinoma cell line
BLI	= bioluminescence imaging
CrC	= critical concentration
DMAP	= 4-dimethylaminopyridine
DMEM	= dubelcco's modified eagle's medium
DMF	= dimethylformamide
DMSO	= dimethyl sulfoxide
FBS	= fetal bovine serum
GAB	= glycerol-assembling buffer
GTP	= guanosine triphosphate
HT-29	= human colorectal adenocarcinoma cell line
IG ₅₀	= half cell growth inhibitory concentration
LD ₅₀	= median lethal dose
LM2	= fibroblastoid mammary carcinoma cell line
MCF-7	= human breast adenocarcinoma cell line
MDA-MB-231	= human breast adenocarcinoma cell line
MTT	= 3-(4,5-dimethylthiazol-2-yl)-2,5-diphenyltetrazolium bromide
NMR	= nuclear magnetic resonance
PBS	= phosphate buffered saline

RT-qPCR	= real time quantitative polymerase chain reaction
SCID	= severe combined immunodeficiency
VDA	= vascular disrupting agent
VEGF	= vascular endothelial growth factor receptor

HUMAN AND ANIMAL RIGHTS

The authors state that all studies were done in compliance with the ethical guidelines for animal welfare of KU Leuven (P277/215).

CONSENT FOR PUBLICATION

Not applicable.

CONFLICT OF INTEREST

This research has been funded by the Ministerio de Economía y Competitividad (project CTQ2014-52949-P), by the Universitat Jaume I (project PI-1B2015-75) and by the Conselleria d'Educació, Investigació, Cultura i Sport de la Generalitat Valenciana (project PROMETEO 2013/027).

ACKNOWLEDGEMENTS

A. M.-M. thanks the Conselleria d'Educació, Investigació, Cultura i Esport de la Generalitat Valenciana for a Ph. D. grant. L. C.-M. thanks Spanish Ministry of Education, Culture and Sport for a FPU fellowship (FPU14/00878). The authors are also grateful to the SCIC of the Universitat Jaume I for providing NMR and Mass Spectrometry facilities.

SUPPORTIVE/SUPPLEMENTARY MATERIAL

Supplementary Material includes:

- General chemical procedures.
- Experimental procedure for the synthesis of colchicine analogues **1-10**, **21-25** and **31-32**.
- Spectral characterization of colchicine analogues **1-10**, **21-25** and **31-32**.
- Experimental procedure for N-Boc deprotection: synthesis of compounds **11-20**, **26-30** and **33-34**.
- Spectral characterization of compounds **11-20**, **26-30** and **33-34**.
- ¹H and ¹³C NMR spectra of all new synthetic compounds.

REFERENCES

- [1] (a) Jordan, M.A.; Wilson, L. Microtubules as a target for anticancer drugs. *Nat. Rev. Cancer* **2004**, *4*, 253-265. (b) Dumontet, C.; Jordan, M.A. Microtubule-binding agents: a dynamic field of cancer therapeutics. *Nat. Rev.*

- Drug Discov.* **2010**, *9*, 790-803. (c) Stanton, R.A.; Gernert, K.M.; Nettles, J.H.; Aneja, R. Drugs that target dynamic microtubules: a new molecular perspective. *Med. Res. Rev.* **2011**, *31*, 443-481. (d) Mukhtar, E.; Adhami, V.M.; Mukhtar, H. Targeting microtubules by natural agents for cancer therapy. *Mol. Cancer Ther.* **2014**, *13*, 275-284. (e) van Vuuren, R.J.; Visagie, M.H.; Theron, A.E.; Joubert, A.M. Antimitotic drugs in the treatment of cancer. *Cancer Chemother. Pharmacol.* **2015**, *76*, 1101-1112.
- [2] Jordan, M.A.; Kamath, K. How do microtubule-targeted drugs work? *Curr. Cancer Drug Targets* **2007**, *7*, 730-742.
- [3] Pandey, D.K.; Tabarak Malik, T.; Dey, A.; Singh, J.; Banik, R.M. Improved growth and colchicine concentration in *Gloriosa superba* on mycorrhizal inoculation supplemented with phosphorus-fertilizer. *Afr. J. Tradit. Complement. Altern. Med.* **2014**, *11*, 439-446.
- [4] Ozkaya, N.; Yalçinkaya, F. Colchicine treatment in children with familial Mediterranean fever. *Clin. Rheumatol.* **2003**, *22*, 314-317.
- [5] (a) Ravelli, R.B.; Gigant, B.; Curmi, P.A.; Jourdain, I.; Lachkar, S.; Sobel, A.; Knossow M. Insight into tubulin regulation from a complex with colchicine and a stathmin-like domain. *Nature* **2004**, 428, 198-202. (b) Bhattacharyya, B.; Anda, D.; Gupta, S.; Banerjee, M. Anti-mitotic activity of colchicine and the structural basis for its interaction with tubulin. *Med. Res. Rev.* **2008**, *28*, 155-183.
- [6] For recent reports on new colchicine derivatives see: (a) Chang, D.J.; Kim, W.J. Discovery of structurally simplified analogs of colchicine as an immunosuppressant. *Bioorg. Med. Chem. Lett.* **2014**, *24*, 3121-3125. (b) Huczynski, A.; Rutkowski, J.; Popiel, K.; Maj, E.; Wietrzyk, J.; Stefanska, J.; Majcher, U.; Bartl, F. Synthesis, antiproliferative and antibacterial evaluation of C-ring modified colchicine analogues. *Eur. J. Med. Chem.* **2015**, *90*, 296-301. (c) Singh, B.; Kumar, A.; Joshi, P.; Guru, S.K.; Kumar, S.; Wani, Z.A.; Mahajan, G.; Hussain, A.; Qazi, A.K.; Kumar, A.; Bharate, S.S.; Gupta, B.D.; Sharma, P.R.; Hamid, A.; Saxena, A.K.; Mondhe, D.M.; Bhushan, S.; Bharate, S.B.; Vishwakarma, R.A. Colchicine derivatives with potent anticancer activity and reduced P-glycoprotein induction liability. *Org. Biomol. Chem.* **2015**, *13*, 5674-5689. (d) Thomopoulou, P.; Sachs, J.; Teusch, N.; Mariappan, A.; Gopalakrishnan, J.; Schmalz, H-G. New colchicine-derived triazoles and their influence on cytotoxicity and microtubule morphology. *ACS Med. Chem. Lett.* **2016**, *7*, 188-191.
- [7] Cosentino, L.; Redondo-Horcajo, M.; Zhao, Y.; Santos, A.R.; Chowdury, K.F.; Vinader, V.; Abdallah, Q.M.A.; Abdel-Rahman, H.; Fournier-Dit-Chabert, J.; Shnyder, S.D.; Loadman, P.M.; Fang, W.; Díaz, J.F.; Barasoain, I.; Burns, P.A.; Pors, K. Synthesis and biological evaluation of colchicine B-ring analogues tethered with halogenated benzyl moieties. *J. Med. Chem.* **2012**, *55*, 11062-11066.
- [8] (a) Hanahan, D.; Weinberg, R.A. The hallmarks of cancer. *Cell* **2000**, *100*, 57-70. (b) Hanahan, D.; Weinberg, R.A. Hallmarks of cancer: the next generation. *Cell* **2011**, *144*, 646-674.
- [9] von Rahden, B.H.A.; Stein, H.J.; Oppermann, F.P.; Sarbia, M. c-MYC Amplification is frequent in Esophageal Adenocarcinoma and Correlated with upregulation of VEGF-A expression, *Neoplasia*, **2006**, *8*, 702-707.
- [10] (a) Vilanova, C.; Díaz-Oltra, S.; Murga, J.; Falomir, E.; Carda, M.; Marco, J.A. Inhibitory effect of pironetin/colchicine hybrids on the expression of the VEGF, hTERT and c-MYC genes, *Bioorg. Med. Chem. Lett.* **2015**, *25*, 3194-3198. (b) Marzo-Mas, A.; Murga, J.; Falomir, E.; Carda, M.; Marco, J.A. Effects on tubulin polymerization and down-regulation of c-Myc, hTERT and VEGF genes by colchicine haloacetyl and haloaroyl derivatives, *Eur. J. Med. Chem.* **2018**, *150*, 591-600.
- [11] For some reports on the inclusion of amino acidic moieties into bioactive molecular scaffolds as an approach for the design of anticancer agents see: (a) Furlan A.; Colombo, F.; Kover, A.; Issaly, N.; Tintori, C.; Lucill, A.; Leroux, V.; Letard, S.; Amat, M.; Asses, Y.; Maignet, B.; Dubreil, P.; Botta, M.; Dono, R.; Bosch, J.; Piccolo, O.; Passarella, D.; Duvia, F. Identification of new aminoacid amides containing the imidazo[2,1-b]benzothiazole-2-ylphenyl moiety as inhibitors of tumorigenesis by oncogenic Met signaling *Eur. J. Med. Chem.* **2012**, *47*, 239-254; (b) Maccallini, C.; Di Matteo, M.; Gallorini, M.; Montagnani, M.; Graziani, V.; Ammazalorso, A.; Amoia, P.; De Filippis, B.; Silvestre, S.D.; Fantacuzzi, M.; et al. Discovery of N-{3-[(ethanimidoylamino)methyl]benzyl}-L-prolinamide dihydrochloride: A new potent and selective inhibitor of the inducible nitric oxide synthase as a promising agent for the therapy of malignant glioma. *Eur. J. Med. Chem.* **2018**, *152*, 53-64; (c) Compound **3** and **13** are described in: Smith, R.L.; Åstrand, O.A.; Nguyen, L.M.; Elvestrand, T.; Hagelin G.; Solberg, R.; Johansen, H.T.; Rongved, P. Synthesis of a novel legumain-cleavable colchicine prodrug with cell-specific toxicity. *Bioorganic & Medicinal Chemistry* **2014**, *22*, 3309-3315.
- [12] Compound **I** has been prepared following the synthetic procedure described in Bagnato, J.D.; Eilers, A.L.; Horton, R.A.; Grissom, C.B. Synthesis and characterization of a cobalamin-colchicine conjugate as a novel tumortargeted cytotoxin, *J. Org. Chem.* **2004**, *69*, 8987-8996.
- [13] Iwaszkiewicz-Grzes, D.; Cholewinski, G.; Kot-Wasik, A.; Trzonkowski, P.; Dzierzbicka, K. Synthesis and biological activity of mycophenolic acid-amino acid derivatives *Eur. J. Med. Chem.* **2013**, *69*, 863-871.
- [14] Liu, Y.; Zhao, C.; Bergbreiter, D.E.; Romo, D. Simultaneous Deprotection and Purification of BOC-amines Based on Ionic Resin Capture *J. Org. Chem.* **1998**, *63*, 3471-3473.
- [15] Rodríguez-Nieto, S.; Medina, M.A.; Quesada, A.R. A re-evaluation of fumagillin selectivity towards endothelial cells, *Anticancer Res.* **2011**, *21*, 3457-3460.
- [16] Hulpia, F.; Noppen, S. Schols, D.; Andrei, G.; Snoeck, R.; Liekens, S.; Vervaeke, P.; Calenbergh, S. Synthesis of a 3'-C-ethynyl-β-d-ribofuranose purine nucleoside

- library: Discovery of a C7-deazapurine analogs as potent antiproliferative nucleosides, *Eur. J. Med. Chem.* **2018**, *157*, 248-267.
- [17] Minn, A.J.; Gupta, G.P.; Siegel, P.M.; Bos, P.D.; Shu, W.; Giri, D.D.; Viale, A.; Olshen, A.B.; Gerald, W.L.; Massagué, J. Genes that mediate breast cancer metastasis to lung, *Nature* **2005**, *436*, 518-524.
- [18] Lancaster, O.M.; Le Berre, M.; Dimitracopoulos, A.; Bonazzi, D.; Zlotek-Zlotkiewicz, E.; Picone, R.; Duke, T.; Piel, M.; Bau, B. Mitotic Rounding Alters Cell Geometry to Ensure Efficient Bipolar Spindle Formation, *Dev. Cell* **2013**, *25*, 270-283.
- [19] Welti, J.; Loges, S.; Dimmeler, S.; Carmeliet, P. Recent molecular discoveries in angiogenesis and antiangiogenic therapies in cancer, *J. Clin. Invest.* **2013**, *123*, 3190-3200.